# Magic angle effect plays a major role in both T1rho and T2 relaxation in articular cartilage

Shao, H ; Pauli, C ; Li, S ; Ma, Y ; Tadros, A S ; Kavanaugh, A ; Chang, E Y ; Tang, G ; Du, J

Abstract: PURPOSE To investigate the effect of sample orientation on T1rho and T2 values of articular cartilage in histologically confirmed normal and abnormal regions using a whole-body 3T scanner. MATERIALS AND METHODS Eight human cadaveric patellae were evaluated using a 2D CPMG sequence for T2 measurement as well as a 2D spin-locking prepared spiral sequence and a 3D magnetization-prepared angle-modulated partitioned-k-space spoiled gradient echo snapshots (3D MAPSS) sequence for T1rho measurement. Each sample was imaged at six angles from 0° to 100° relative to the B0 field. T2 and T1rho values were measured for three regions (medial, apex and lateral) with three layers (10% superficial, 60% middle, 30% deep). Multiple histopathologically confirmed normal and abnormal regions were used to evaluate the angular dependence of T2 and T1rho relaxation in articular cartilage. RESULTS Our study demonstrated a strong magic angle effect for T1rho and T2 relaxation in articular cartilage, especially in the deeper layers of cartilage. On average, T2 values were increased by 231.8% (72.2% for superficial, 237.6% for middle, and 187.9% for deep layers) while T1rho values were increased by 92% (31.7% for superficial, 69% for middle, and 140% for deep layers) near the magic angle. Both normal and abnormal cartilage showed similar T1rho and T2 magic angle effect. CONCLUSIONS Changes in T1rho and T2 values due to the magic angle effect can be several times more than that caused by degeneration, and this may significantly complicate the clinical application of T1rho and T2 as an early surrogate marker for degeneration.

DOI: https://doi.org/10.1016/j.joca.2017.01.013

HHS Public Access

Author manuscript

*Osteoarthritis Cartilage*. Author manuscript; available in PMC 2017 December 15.

Published in final edited form as:

*Osteoarthritis Cartilage*. 2017 December ; 25(12): 2022–2030. doi:10.1016/j.joca.2017.01.013.

# Magic Angle Effect Plays a Major Role in Both T1rho and T2 Relaxation in Articular Cartilage

**Hongda Shao**[1,2], **Chantal Pauli**[3], **Shihong Li**[1,4], **Yajun Ma**[1], **Anthony S. Tadros**[1], **Eric Y. Chang**[5,1], **Guangyu Tang**[2], and **Jiang Du**[1]

[1]Department of Radiology, University of California, San Diego, CA [2]Department of Radiology, Shanghai Tenth People's Hospital, Tongji University School of Medicine, Shanghai, China [3]Institute for Surgical Pathologie, University Hospital Zurich, Zurich, Switzerland [4]Department of Radiology, Huadong Hospital, Fudan University, Shanghai, China 200040 [5]Radiology Service, VA San Diego Healthcare System, San Diego, CA

## Abstract

**PURPOSE—**To investigate the effect of sample orientation on T1rho and T2 values of articular cartilage in histologically confirmed normal and abnormal regions using a whole-body 3T scanner, providing information on the angular dependence of T1rho and T2 in clinical imaging.

**MATERIALS AND METHODS—**Eight human cadaveric patellae were evaluated using a 2D CPMG sequence for T2 measurement as well as a 2D spin-locking prepared spiral sequence and a 3D magnetization-prepared angle-modulated partitioned-k-space spoiled gradient echo snapshots (3D MAPSS) sequence for T1rho measurement. Each sample was imaged at six angles from 0° to 100° relative to the $B_0$ field. T2 and T1rho values were measured for three regions (medial, apex and lateral) with three layers (10% superficial, 60% middle, 30% deep). Multiple histopathologically confirmed normal and abnormal regions were also used to evaluate the angular dependence of T2 and T1rho relaxation in articular cartilage.

**RESULTS—**Our study demonstrated a strong magic angle effect for T1rho and T2 relaxation in articular cartilage, especially in the deeper layers of cartilage. On average over eight patellae, T2 values were increased by 231.8% (72.2% for superficial, 237.6% for middle, and 187.9% for deep layers) while T1rho values were increased by 92% (31.7% for superficial, 69% for middle, and 140% for deep layers) near the magic angle. Both normal and abnormal cartilage showed similar T1rho and T2 magic angle effect.

Corresponding Address: Jiang Du, jiangdu@ucsd.edu, University of California, San Diego, Department of Radiology, 200 West Arbor Drive, San Diego, CA 92103-8756, Phone (619) 471-0786, Fax (619) 471-0503.

**Author Contributions**

HS, CP, YM, EYC, GT and JD designed the study; HS and JD performed the study; HS, YM and JD analyzed data; HS, CP, YM, AT, EYC, GT and JD wrote the manuscript.

**Conflict of interest**

The authors of this work have no conflicts of interest to report relevant to this work.

**CONCLUSIONS—**Changes in T1rho and T2 values due to the magic angle effect can be several times more than that caused by degeneration, and this may significantly complicate the clinical application of T1rho and T2 as an early surrogate marker for degeneration.

### Keywords

T1rho; T2; magic angle; degeneration; articular cartilage

## Introduction

Osteoarthritis (OA) affects over 30 million Americans and has a substantial impact on the health care system with a cost estimated at over $60 billion per year (1). Magnetic resonance imaging (MRI) is routinely used for the characterization of advanced cartilage lesions such as defects or fissures. However, conventional morphological MRI techniques are less sensitive to the early stages of OA when cartilage is still present (2). There is increasing need to improve the detection of OA at this early stage to allow timely intervention prior to irreversible damage or complete loss of tissue. The most important early biochemical and microscopic signs of OA include loss of proteoglycans (PGs), and changes in collagen microstructure and water content (3).

Quantitative MRI has the potential to identify cartilage tissue components that change in the early stages of OA. In recent years, T2 and T1rho have been widely investigated as biomarkers for OA (4–9). T2 has been shown to be sensitive to degradation of the collagen matrix (4,5), while T1rho has been shown to be sensitive to changes in PG content (6). The magic angle effect is an extraneous variable which can contribute to changes in both T2 and T1rho, thus complicating evaluation of joint tissue degeneration (5). The ordered collagen fibers in joint tissues are associated with dipole-dipole interactions, which are modulated by the term $3\cos^2\theta$-1 (10). The dipole-dipole interactions are minimized when θ, which is the angle between the collagen fiber orientation and the main magnetic field $B_0$, equals approximately 55° or 125°. At these angles, T2 and T1rho values are often increased relative to those obtained with fibers parallel to the main magnetic field (11–13).

While the magic angle effect in T2 relaxation is well understood, the literature regarding T1rho relaxation mechanisms is somewhat inconsistent (11–16). For example, Mlynarik et al. measured relaxation rates in the rotating frame (R1rho) and spin-spin relaxation rates (R2) in articular cartilage, and concluded that the dominant T1rho relaxation mechanism at $B_0$ ≤3T is a dipolar interaction due to slow anisotropic motion of water molecules in the collagen matrix (11). Menezes et al. drew similar conclusions and reported that changes in collagen concentration alone could fully account for the variation in T1rho seen in human tissue (14). Wang et al. reported a significant magic angle effect in T1rho relaxation, as well as a bi-component T1rho decay when the fibers were parallel to $B_0$ and a single-component T1rho decay when the sample was 54° relative to $B_0$ (13). Meanwhile, Akella et al. reported that spin-lock radiofrequency (RF) pulses could reduce the laminar appearance of articular cartilage, with residual dipolar interaction from motionally-restricted water making a significant contribution to T1rho dispersion (15). More recently, Li et al. investigated the

effect of angular orientation on T1rho and T2 values, and found a relatively small angular dependence (16).

Most of the studies demonstrating a strong angular dependence in T1rho relaxation in articular cartilage were performed on high performance NMR spectrometers (11–14), while those showing weak angular dependence were performed on clinical whole-body scanners (15,16). Since NMR spectrometers and clinical MR scanners have very different RF powers and gradient strengths, it is necessary to further investigate the angular dependence of T1rho relaxation in articular cartilage systematically using a clinical whole-body MR scanner. This would help elucidate the role of the magic angle effect in a clinical setting. Furthermore, the magic angle effects in normal and abnormal articular cartilage are still unknown.

In this study, we aimed to further evaluate the effect of sample orientation on T1rho and T2 values of articular cartilage from cadaveric human patellae. Magic angle effects in histologically confirmed normal and abnormal regions were systematically investigated using a whole-body 3T scanner, providing information on the angular dependence of T1rho and T2 in clinical imaging.

## Materials and Methods

### Human patellae procurement

Eight fresh human patellae from eight donors (5 males, age range = 48 – 90, mean ± standard deviation of 63.4 ± 16.0 years; 3 females, age range = 50 – 92, 74.3 ± 21.8 years) were obtained from tissue banks approved by our Institutional Review Board. After harvesting, a transverse slab of ~5 mm thickness was cut from the specimens using a low-speed diamond saw (Isomet 1000, Buehler) with constant water irrigation, and stored in a phosphate buffered saline (PBS) soaked gauze at 4°C prior to MR imaging.

### MR data acquisition

All data acquisitions were performed with a 3T MRI system (Signa HDx, GE Healthcare, Waukesha, WI, USA) with a maximum gradient strength of 40 mT/m and a maximum slew rate of 150 mT/m/ms. A 3-inch receive-only surface coil was used for signal reception (body coil was used for signal excitation). Patella samples were placed in perfluorooctyl bromide (PFOB) solution to minimize susceptibility effects at tissue-air junctions. A single slice at the center of each patella sample was imaged. The imaging protocol is shown in Table 1, which included the following three sequences: 1) a standard clinical two-dimensional (2D) Carr-Purcell-Meiboom-Gill (CPMG) sequence with eight echoes (10 to 80 ms) for T2 measurement; 2) a 2D spin-locking prepared spiral sequence for T1rho measurement (8); 3) a 3D magnetization-prepared angle-modulated partitioned-*k*-space spoiled gradient echo snapshots (3D MAPSS) sequence for T1rho measurement (9). Typical imaging parameters included: field of view (FOV) = 5 cm, matrix = 256×256, 2 mm slice thickness, spin-locking time (TSL) = 0, 10, 20, 40, 80 ms for 2D and 3D T1rho measurement, and TE = 10, 20, 30, 40, 50, 60, 70, 80 ms for CPMG T2 measurement. A spin-locking field strength of 500 Hz was used for both 2D and 3D T1rho imaging. A TR of 1500 ms was used for 2D spiral T1rho imaging and a TR of 2000 ms was used for CPMG imaging. The scan time was

around 10 minutes for each sequence. The same imaging protocol was applied to each sample at six different angular orientations: 0°, 20°, 40°, 60°, 80° and 100° relative to the $B_0$ field, which took about ~9 hours for each patella specimen. At 0°, the apex of each patella was oriented parallel to the main magnetic field $B_0$. Data acquisition at 0° was repeated twice, once at the beginning and once at the end of the scan to investigate potential tissue degeneration due to the long imaging protocol (~10.5 hours). One patella sample was scanned three times on three different days to examine reproducibility using the CPMG T2, spiral T1rho and MAPSS T1rho sequences.

## Tissue processing

After MRI scans, each patella slab was immediately fixed in Z-Fix (Anatech, Battle Creek, MI) for three days followed by decalcification in TBD-2 (Thermo Scientific, Kalamazoo, MI). The center of each patella slab was marked with a tissue marking dye (Cancer Diagnostics, Morrisville, NC) on the lateral and medial edges in order to provide orientation. After complete decalcification, dehydration with alcohol, immersion in Pro-Par Clearant (Anatech LTD, Battle Creek, MI), and infiltration with paraffin (Paraplast, McCormick Scientific, Richmond, IL), transverse sections covering the cartilage and subchondral bone were obtained. Each tissue block was then trimmed on a microtome using the orientation marks for reference. Finally, sections of 5 μm thickness were cut at the defined central location to match the MRI scans. Several sections from each patella slab were stained with Safranin O-Fast Green for histopathology.

## Histopathology

Standard histopathology was performed on each patella slab after fixation. First, Safranin O-Fast Green staining was applied to each sectioned slide. Then the stained slide was scanned with a Leica SCN4000 slide scanner (Leica Microsystems, Buffalo Grove, IL) and viewed with SlidePath software (Leica Microsystems, Buffalo Grove, IL). Since the patella slab might contain several regions with different histopathologic grades, multiple regions were chosen to cover different grades within each specimen. This was accomplished using 1–3 regions of interest (ROIs) per patella, chosen for Spearman rank correlation between histopathological grading and MRI T2 and T1rho measurements. Each ROI was given a Mankin score ranging from 0 to 14 by an experienced musculoskeletal histopathologist (CP with 8 years of experience with a primary focus on articular cartilage), who was blinded to the MRI results (17). The ROI was chosen to cover each focal lesion and include the whole cartilage depth from the superficial to the deep radial layers. For simplicity, all ROIs were classified as normal or abnormal. A Mankin score of equal or less than 2 was considered normal, while a Mankin score of greater than 2 was considered abnormal.

## Post-processing and image analysis

CPMG T2, spiral T1rho and MAPSS T1rho datasets acquired at six different angular orientations were first manually aligned using ImageJ software, and then automatically registered using FLIRT (Functional MRI of the Brain's Linear Image Registration Tool) software using six parameter rigid body model and correlation ratio as the cost function (18).

T1rho and T2 analysis algorithms were written in MATLAB (Mathworks Inc., Natick, MA). The T1rho and T2 values were determined using nonlinear least square mono-exponential curve fitting of average signal intensity from three regions (medial, apex and lateral) with three layers (10% superficial, 60% middle, 30% deep) as well as a global ROI comprising the entire region. The semi-automated home-developed MATLAB program allowed copying and pasting of ROIs to the registered images. This technical approach ensured that ROIs were identically located on images obtained at different angles and sequences. Multiple histopathologically confirmed normal and abnormal regions in each patella were used for analysis. The number of regions was determined by one author (CP) depending on the grade of OA severity. These ROIs were also subject to 2D and 3D T1rho as well as CPMG T2 analyses. To investigate the magic angle effect, the maximal and minimal mean T1rho and T2 values for different layers as well as the global ROIs were calculated for normal and abnormal cartilage.

### Statistical analysis

Goodness of fit statistics, including the R-squared value and standard error or fitting confidence level, were calculated. Fit curves along with their 95% confidence intervals (CI) and residual signal curves were created. The fitted T1rho and T2 values were correlated with Mankin scores. Spearman rank correlation was used, and its statistical significance assessed. Since multiple measurements were obtained from the same donor, non-parametric bootstrap was used to assess the significance of the Spearman correlation (19). The resampling in bootstrap replicates was done per-subject, to adjust for within-subject dependence. Significance of the correlation was assessed based on the bias-corrected, accelerated bootstrap confidence interval (CI) around the correlation coefficient. The p-values for the correlations were calculated based on the bootstrap. A p-value of less than 0.05 was considered statistically significant.

## Results

The average coefficients of variation for quantitative analysis of one patella sample on three repeated acquisitions were 3.4% for CPMG T2 measurement, 2.1% for 2D spiral T1rho measurement, and 2.7% for 3D MAPSS T1rho measurement. These results show that all three quantitative measurement techniques provide reliable estimation of T2 and T1rho values of articular cartilage. T1rho values measured at the beginning and end of the magic angle study (~10.5 hours scan) varied by less than 5.0%, suggesting minor tissue degeneration in PFOB.

Selected 2D spiral T1rho images of a histologically confirmed normal patella acquired at three different angular orientations of 0°, 40° and 80° relative to the $B_0$ field are shown in Figure 1. The middle and deep layers of articular cartilage showed dramatic signal change: near zero signal when the collagen fibers were oriented parallel to the $B_0$ field (arrows in Figure 1E) and high signal when the fibers were oriented near the magic angle (arrows in Figure 1I and 1M). The superficial layers of articular cartilage showed relatively less signal change as a function of angular orientation.

Quantitative analysis of 2D spiral T1rho values of the superficial, middle and deep layers of articular cartilage, as well as a global ROI in the apex region (arrows in Figure 1), at three different angular orientations are shown in Figure 2. T1rho values were lowest when radial fibrils were near 0° relative to $B_0$ (18.2 ± 0.6 ms for the deep layer, 38.7 ± 0.6 ms for the middle layer, 56.5 ± 0.9 ms for the superficial layer, 33.5 ± 0.6 ms for the global ROI) and increased to a maximum when radial fibrils were near 60° relative to $B_0$ (51.7 ± 0.8 ms for the deep layer, 69.3 ± 0.9 ms for the middle layer, 86.2 ± 2.5 ms for the superficial layer, 64.1 ± 1.2 ms for the global ROI). 3D MAPSS T1rho values were very close to those of 2D spiral T1rho values, with less than 10% difference. For a global ROI T2 values exhibited similar angle-dependency: ~33.2 ms near 0°, ~82.1 ms near the magic angle, and ~59.6 ms near 90° relative to $B_0$.

Figure 3 shows the change in T1rho and T2 values across varying angle orientations; ROIs corresponding to the deep, middle and superficial layers are presented for the lateral, apex and medial regions of the same normal patella shown in Figure 1. A significant magic angle effect in both T1rho and T2 is clearly demonstrated for all three layers in all three regions, with maximal angular dependence for the deep and middle layers, and much less degree of angular dependence for the superficial layers.

Figure 4 shows selected 2D spiral T1rho images and 2D CPMG T2 images of another normal patella at two different angular orientations of 0° and 60° relative to the $B_0$ field. Again, a strong magic angle effect was observed (arrows). T1rho showed a similar pattern of angular dependence as T2, further demonstrating its sensitivity to the magic angle effect.

Figure 5 shows a patella sample with histologically confirmed normal regions in the medial and apex regions as well as an abnormal region in the lateral region with a Mankin score of 7. Strong magic angle effect was observed for both T1rho and T2 in the normal region. The abnormal region showed reduced magic angle effect, especially for T1rho relaxation.

Table 2 shows the averaged magic angle effects in T1rho and T2 relaxation times for normal (Mankin score $\leq 2$) and abnormal (Mankin score $\geq 3$) cartilage specimens, as well as the standard deviation. 2D spiral T1rho values from global ROIs were increased by 72% for normal cartilage and 63% for abnormal cartilage. 3D MAPSS T1rho values from global ROIs were increased by 67% for normal cartilage and 53% for abnormal cartilage. T2 values from global ROIs were increased by 158% for normal cartilage and 104% for abnormal cartilage. Similar changes were observed for both T1rho and T2 for different layers of articular cartilage. In general, abnormal cartilage showed slightly less (4~10%) magic angle effect.

Correlation between histopathological grading and T2, spiral T1rho and MAPSS T1rho is presented in Figure 6. There is little correlation between T2 and the Mankin score (Rho = 0.29; P = 0.17) and low correlation between 2D spiral T1rho (Rho = 0.47; P = 0.06) and 3D MAPSS T1rho (Rho = 0.42; P = 0.06) and the Mankin score. The low correlation is most likely due to the strong magic angle effect in both T2 and T1rho relaxation times, as demonstrated in Table 2.

## Discussion

The biomechanical properties of articular cartilage are highly related to the composition of the extracellular matrix, which is composed of type II collagen with intertwined PGs. The architectural and molecular structures, as well as concentrations of collagen and PGs, are important parameters when evaluating articular cartilage. A series of techniques have been developed for this purpose, including T2 and T1rho. The magic angle effect on T2 is well known (5,10). However, the literature regarding T1rho relaxation mechanisms is inconsistent, with some groups finding strong residual dipolar interaction (11–14,20), and other groups reporting a reduced magic angle effect (15,16). Our study indicates that the magic angle effect plays a significant role in not only T2 relaxation, but T1rho relaxation. Global T1rho was increased by ~70% for normal articular cartilage and 50 – 60% for abnormal cartilage. In contrast, moderate degeneration lead to a T1rho increase of less than 20%, which is far less than that induced by the magic angle effect. T2 showed significantly higher magic angle effect than T1rho. T2 for a global ROI was increased by 156% for normal articular cartilage and 104% for abnormal articular cartilage, nearly twice the increase in T1rho relaxation times for both normal and abnormal cartilage. The superficial layers showed relatively less magic angle effect, while the middle and deep layers showed markedly increased magic angle effect for both T1rho and T2 relaxation times.

Our study shows more magic angle effect in T1rho relaxation in articular cartilage than reported in recent studies. Akella et al. investigated the influence of RF spin-lock pulse on the laminar appearance of bovine cartilage, which has more organized collagen fibers with less complex structures than that of human cartilage (15). They observed strong laminar appearance in T2-weighted images but absence of laminar appearance in T1rho-weighted images with a spin-lock field strength of 500 Hz. They concluded that the residual dipolar coupling constant in cartilage was less than 500 Hz. T1rho became angular independent when the spin-lock field strength was stronger than 2 kHz. T1rho was about 25% higher when the fiber was oriented 55° to the $B_0$ field over parallel orientation. More recently, Li et al. investigated the angular dependence of T1rho and T2 relaxation times in cadaveric human femoral-tibial cartilage (16). They observed only a minor magic angle effect, with less than 21% increase for T2 (from 47.3 ± 13.3 ms at 0° to 57.4 ± 11.6 ms at 54°) and 16% for T1rho (from 59.4 ± 9.2 ms at 0° to 68.8 ± 4.7 ms at 54°) at 500 Hz. They only observed a moderate correlation between R1rho (1/T1rho) and PG contents ($R = 0.45$, $P = 0.002$), which might be due to the magic angle effect (16). Wang et al. reported a bi-component T1rho decay when the fibers were oriented 0° relative to $B_0$ (39.8 ± 3.0 ms and 94.1 ± 2.8 ms with a fraction of 18.8% and 81.2%, respectively) and a single-component T1rho decay when the fibers were 54° relative to $B_0$ (105.4 ± 2.2 ms) (13). This orientation dependent multi-component behavior in T1rho relaxation in cartilage further complicates the interpretation of T1rho relaxation.

Our results using a whole-body clinical 3T MR scanner are largely inconsistent with the results by Mlynarik et al., who conducted a systematic study on T1rho relaxation mechanisms in articular cartilage using high performance NMR spectrometers at two field strengths: 2.95 T and 7 T (11). At 2.95 T, T1rho increased by 62% for the radial zone and 5% for the transitional zone due to the magic angle effect. Results from the Mlynarik study

suggest that the dominant T1rho and T2 relaxation mechanisms at 3T or lower field strength is the dipolar interaction. Furthermore, they found negligible T1rho dispersion between 300 Hz and 2500 Hz in the transitional zone, suggesting that exchange between OH and NH protons with water is unlikely a dominant contributor to the scalar relaxation.

The mechanisms contributing to T1rho relaxation include dipolar interactions, scalar coupling and chemical exchange processes. The strong angular dependence in T1rho relaxation is very similar to that in T2 relaxation in articular cartilage (21), suggesting that the dominating factor is dipolar interactions. The variation in T1rho values amongst different layers of articular cartilage is consistent with the above hypothesis. In the deep radial layers, the collagen fibers are highly organized and radially oriented, leading to very strong dipolar interactions and thus much reduced T1rho values (i.e., around 20 ms). In the middle layer, the collagen fibers are less organized with a mix of radially and obliquely oriented fibers, leading to reduced dipolar interactions and thus longer T1rho values (i.e., around 50 ms). In the superficial layer, the collagen fibers are largely randomly distributed and oriented parallel to the surface, leading to much reduced dipolar interactions and thus much longer T1rho values (i.e., around 80 ms) (21). Special attention should be given when using T1rho to probe macromolecular slow-motion interactions, i.e., minimizing angular dependence by comparing T1rho from regions of articular cartilage with similar collagen fiber orientations. Some studies show that T1rho is a sensitive marker for detecting PG changes in articular cartilage (6,22), likely because they were comparing T1rho values of cartilage with similar fiber orientations.

The strong angular dependence of T1rho relaxation may explain the inconsistencies in the literature regarding the correlation of T1rho with cartilage degeneration. Menezes et al. reported no correlation between T1rho and PG concentration in cartilage (14). Their results also showed that T1rho is sensitive to collagen content, which may have a greater impact on T1rho than PG content. Wheaton et al. reported a strong correlation between T1rho and PG content ($R2 = 0.926$) in one ex vivo study (23), however, the agreement between T1rho and arthroscopically documented cartilage degeneration was only modest for Outerbridge grades 1 and 2 damage (24), likely because ex vivo studies were subject to minimal magic angle effect while in vivo studies of femoral-tibial cartilage were subject to strong magic angle effect. Another study by Regatte et al. showed up to 30 – 120% increase in T1rho values in OA subjects over the control group (25). Li et al. showed a 19% increase in T1rho values in OA subjects over the healthy control group (16). In a multicenter trial, Mosher et al. showed a 4 – 7% increase in T1rho values in mild OA subjects, and a 16 – 35% increase in T1rho values in moderate OA subjects over the healthy control group (26).

Our study suggests that, similar to T2 relaxation, T1rho relaxation is subject to strong magic angle effect, which may significantly complicate its clinical interpretation. Both normal and abnormal articular cartilage showed similar strong magic angle effects, although the abnormal regions showed slightly reduced angular dependence. Similar to the substantial heterogeneity across healthy cartilage seen with T2 (27), T1rho may also require more elaborate definitions for spatial variation (28). T1rho profiles across healthy and abnormal articular cartilage may show a significant difference and might be a useful parameter for clinical interpretation.

There are several limitations to this study. First, only eight specimens were scanned due to the long scan time associated with MR imaging of each specimen. Second, each cadaveric patella was scanned for more than 10 hours, covering six angular orientations using three different sequences. Cartilage degeneration during the scanning process might have changed quantitative MR measurements. However, we measured T1rho at 0° both at the beginning and end of the scan, and found changes less than 5%. Third, patellar cartilage may show a multi-component behavior (13,29,30), but only a single component analysis was performed. Multi-component analysis has a high signal-to-noise ratio demand and may require longer scan time (31), which is difficult with this protocol, which is already 10 hours long. Fourth, the ROIs were chosen by a single person who was blinded to MR imaging, and were registered between MRI and histology sections through visual assessment using landmarks. There is potential for inconsistency in data analysis introduced via this method. Fifth, radiograph and Kellgren-Lawrence (KL) grading was not performed and therefore no correlation was performed between T1rho/T2 and KL score. Sixth, the ROI size is likely to affect the magic angle behavior in both T1rho and T2 relaxation times. However, the ROI sizes are different between the different magic angle studies, complicating the quantitative comparison. Seventh, the magic angle effect in clinical studies of OA patients was not included in this study, and the clinical significance remains to be investigated. Eighth, techniques to minimize the magic angle effect in T1rho relaxation were not investigated in this study. One approach is to increase the spin-locking field strength (15,20), which may also increase the specific absorption ratio (SAR) and thus require longer TR and longer total scan time. Another approach is to use the adiabatic T1rho preparation (32), which is a promising magic angle insensitive technique. The clinical significance of adiabatic T1rho imaging remains to be investigated.

In conclusion, we have shown that there is a significant angular dependence of T1rho relaxation in patellar articular cartilage, with the strongest variation in the deeper layers of cartilage, and reduced variation in the superficial layers of cartilage when evaluated using a clinical 3T MR system. Both normal and abnormal articular cartilage showed strong angular dependence in T1rho relaxation, with slightly less variation in abnormal cartilage.

## Acknowledgments

**Funding source**

The authors acknowledge grant support from GE Healthcare, NIH (1R01 AR062581 and 1R01 AR068987) and the VA Clinical Science R&D Service (1I01CX001388).

## References

1. Andersson, G. American Academy of Orthopaedic Surgeons. The burden of musculoskeletal diseases in the United States: prevalence, societal, and economic cost. Rosemont, IL: American Academy of Orthopaedic Surgeons; 2008.
2. Burstein D, Bashir A, Gray ML. MRI techniques in early stages of cartilage disease. Invest Radiol. 2005; 35:622–638.
3. Buckwalter JA, Martin J. Degenerative joint disease. Clin Symp. 1995; 47:1–32. [PubMed: 7554763]
4. Mosher TJ, Dardzinski BJ. Cartilage MRI T2 relaxation time mapping: overview and applications. Semin Musculoskelet Radiol. 2004; 8:355–368. [PubMed: 15643574]

5. Eckstein F, Burstein D, Link TM. Quantitative MRI of cartilage and bone: degenerative changes in osteoarthritis. NMR in Biomedicine. 2006; 19:822–854. [PubMed: 17075958]
6. Duvvuri U, Reddy R, Patel SD, Kaufman JH, Kneeland JB, Leigh JS. T1rho-relaxation in articular cartilage: effects of enzymatic degradation. Magn Reson Med. 1997; 38:863–867. [PubMed: 9402184]
7. Regatte RR, Akella SVS, Borthakur A, Kneeland JB, Reddy R. In vivo proton MR three-dimensional T1ρ mapping of human articular cartilage: initial experience. Radiol. 2003; 229:269–274.
8. Li X, Han ET, Ma B, Link TM, Newitt DC, Majumdar S. In vivo 3T spiral imaging based multi-slice T1ρ mapping of knee cartilage in osteoarthritis. Magn Reson Med. 2005; 54:929–936. [PubMed: 16155867]
9. Li X, Han ET, Ma B, Busse RF, Majumdar S. In vivo T1ρ mapping in cartilage using 3D magnetization-prepared angle-modulated partitioned k-space spoiled gradient echo snapshots (3D MAPPS). Magn Reson Med. 2008; 59:298–307. [PubMed: 18228578]
10. Xia Y, Farquhar T, Burton-Wurster N, Lust G. Origin of cartilage laminae in MRI. J Magn Reson Imaging. 1997; 7:887–894. [PubMed: 9307916]
11. Mlynarik V, Szomolanyi P, Toffanin R, Vittur F, Trattnig S. Transverse relaxation mechanisms in articular cartilage. J Magn Reson. 2004:300–307. [PubMed: 15261626]
12. Mlynarik V, Trattnig S, Huber M, Zembsch A, Imhof H. The role of relaxation times in monitoring proteoglycan depletion in articular cartilage. J Magn Reson Imaging. 1999; 10:497–502. [PubMed: 10508315]
13. Wang N, Xia Y. Dependencies of multi-component T2 and T1rho relaxation on the anisotropy of collagen fibrils in bovine nasal cartilage. J Magn Reson. 2011; 212:124–132. [PubMed: 21788148]
14. Menezes NM, Gray ML, Hartke JR, Burstein D. T2 and T1ρ MRI in articular cartilage systems. Magn Reson Med. 2004; 51:503–509. [PubMed: 15004791]
15. Akella SVS, Regatte RR, Wheaton AJ, Borthakur A, Reddy R. Reduction of residual dipolar interaction in cartilage by spin-lock technique. Magn Reson Med. 2004; 52:1103–1109. [PubMed: 15508163]
16. Li X, Cheng J, Lin K, Saadat E, Bolbos RI, Ries MD, Horvai A, Link TM, Majumdar S. Quantitative MRI using T1rho and T2 in human osteoarthritis cartilage specimens: correlation with biochemical measurements and histology. Magn Reson Imaging. 2011; 29:324–334. [PubMed: 21130590]
17. Mankin HJ. Biochemical and metabolic aspects of osteoarthritis. Orthop Clin North Am. 1971; 2:19–31. [PubMed: 4940528]
18. Jenkinson M, Bannister P, Brady JM, Smith SM. Improved Optimisation for the Robust and Accurate Linear Registration and Motion Correction of Brain Images. NeuroImage. 2002; 17(2): 825–841. [PubMed: 12377157]
19. Shao J, Kubler J, Pigeot I. Consistency of the bootstrap procedure in individual bioequivalence. Biometrika. 2000; 87:573–585.
20. Du J, Statum S, Znamirowski R, Bydder GM, Chung CB. Ultrashort TE T1rho magic angle imaging. Magn Reson Med. 2013; 26:682–687.
21. Wang N, Badar F, Xia Y. MRI properties of a unique hypo-intense layer in degraded articular cartilage. Phys Med Biol. 2015; 60:8709–8721. [PubMed: 26509475]
22. Regatte RR, Akella SVS, Lonner JH, Kneeland JB, Reddy R. T1ρ relaxation mapping in human osteoarthritis (OA) cartilage: comparison of T1ρ with T2. J Magn Reson Imaging. 2006; 23:547–553. [PubMed: 16523468]
23. Wheaton AJ, Dodge GR, Elliott DM, Nicoll SB, Reddy R. Quantification of cartilage biomechanical and biochemical properties via T1rho magnetic resonance imaging. Magn Reson Med. 2005; 54:1087–1093. [PubMed: 16200568]
24. Witschey WR, Borthakur A, Fenty M, Kneeland BJ, Lonner JH, Mcardle EL, Sochor M, Reddy R. T1rho MRI quantification of arthroscopically confirmed cartilage degeneration. Magn Reson Med. 2010; 63:1376–1382. [PubMed: 20432308]

25. Regatte RR, Akella SV, Lonner JH, Kneeland JB, Reddy R. T1rho relaxation mapping in human osteoarthritis (OA) cartilage: comparison of T1rho with T2. J Magn Reson Imaging. 2006; 23:547–553. [PubMed: 16523468]

26. Mosher TJ, Zhang Z, Reddy R, Boudhar S, Milestone BN, Morrison WB, Kwoh CK, Eckstein F, Witschey WR, Borthakur A. Knee articular cartilage damage in osteoarthritis: analysis of MR image biomarker reproducibility in ACRIN-PA 4001 multicenter trial. Radiology. 2011; 258:832–842. [PubMed: 21212364]

27. Smith HE, Mosher TJ, Dardzinski BJ, Collins BG, Collins CM, Young QX, Schmithorst VJ, Smith MB. Spatial variation in cartilage T2 of the knee. J Magn Reson Imaging. 2001; 14:50–55. [PubMed: 11436214]

28. Li X, Pai A, Blumenkrantz G, Garballido-Gamio J, Link T, Ma B, Ries M, Majumdar S. Spatial distribution and relationship of T1rho and T2 relaxation in knee cartilage with osteoarthritis. Magn Reson Med. 2009; 61:1310–1318. [PubMed: 19319904]

29. Pauli C, Bae WC, Lee M, Lotz M, Bydder GM, Lima D, Chung CB, Du J. Ultrashort echo time (UTE) magnetic resonance imaging of the patella with bi-component analysis: correlation with histopathology and polarized light microscopy. Radiology. 2012; 264:484–493. [PubMed: 22653187]

30. Shao H, Chang EY, Pauli C, Zanganeh S, Bae W, Chung CB, Tang G, Du J. UTE bi-component analysis of T2* relaxation in articular cartilage. Osteoarthritis Cartilage. 2016; 24:364–373. [PubMed: 26382110]

31. Reiter DA, Li PC, Fishbein KW, Spencer RG. Multicomponent T2 relaxation analysis in cartilage. Magn Reson Med. 2009; 61:803–809. [PubMed: 19189393]

32. Rautiainen J, Nissi MJ, Liimatainen T, Herzog W, Kohonen RK, Nieminen MT. Adiabatic rotating frame relaxation of MRI reveals early cartilage degeneration in a rabbit model of anterior cruciate ligament transection. Osteoarthritis and Cartilage. 2014; 22:1444–1452. [PubMed: 25278055]

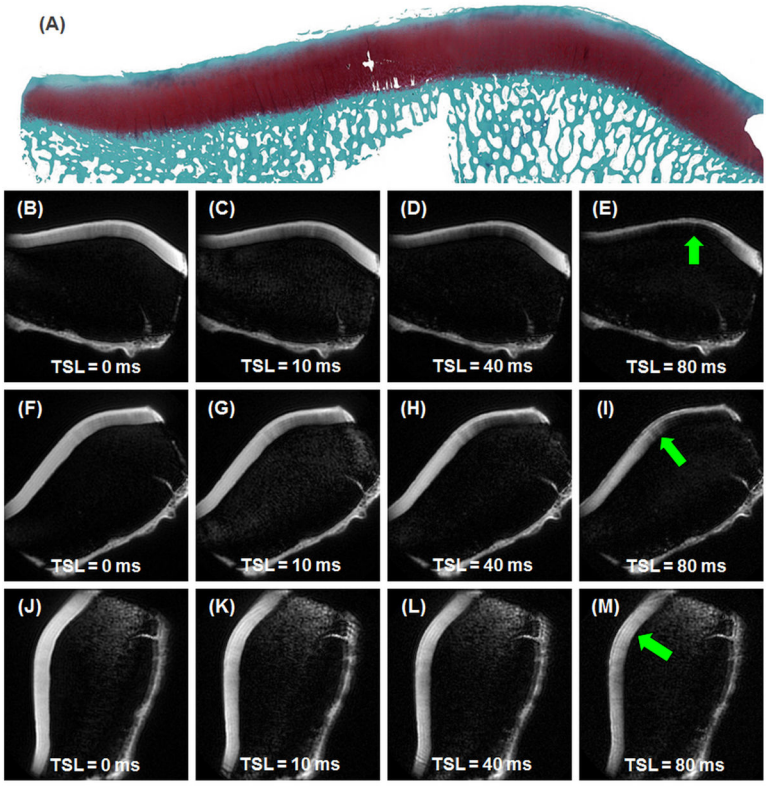


**Figure 1.**

Histology (1st row) and 2D spiral T1rho imaging of normal patellar cartilage. MR images from 0° (2nd row), 40° (3rd row) and 80° (4th row) relative to $B_0$ are shown at increasing TSLs of 0, 10, 40 and 80 ms (left to right). MR signal shows strong angular dependence, most evident in the middle and deep layers of articular cartilage, with minimal signal at 0° (arrow in E) and high signal at 40°and 80° (arrows in I and M, respectively).

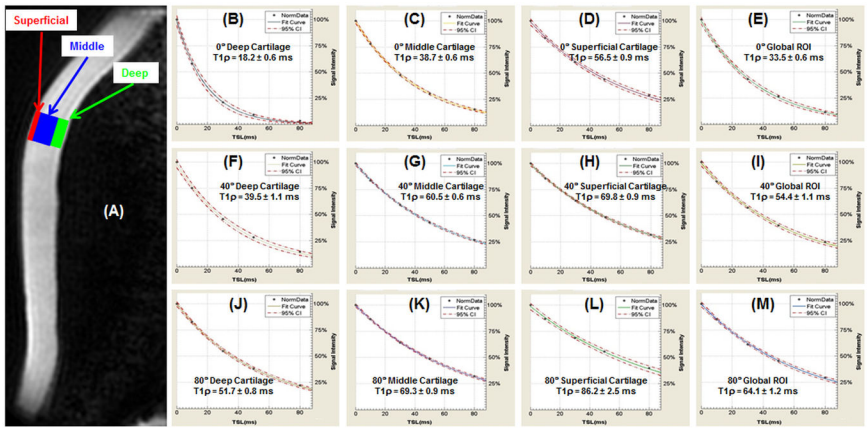


**Figure 2.**

2D spiral T1rho image (A) from Figure 1J shows the three ROIs and a global ROI (all three layers) used for fitting of T1rho at 0° (1st row) for the deep (B), middle (C), and superficial (D) layers of cartilage as well as global ROI (E); at 40° (2nd row) for the deep (F), middle (G), and superficial (H) layers of cartilage as well as global ROI (I); and at 80° (3rd row) for the deep (J), middle (K), and superficial (L) layers of cartilage as well as global ROI (M). T1rho increases from the deep layer to the superficial layer for all angular orientations.

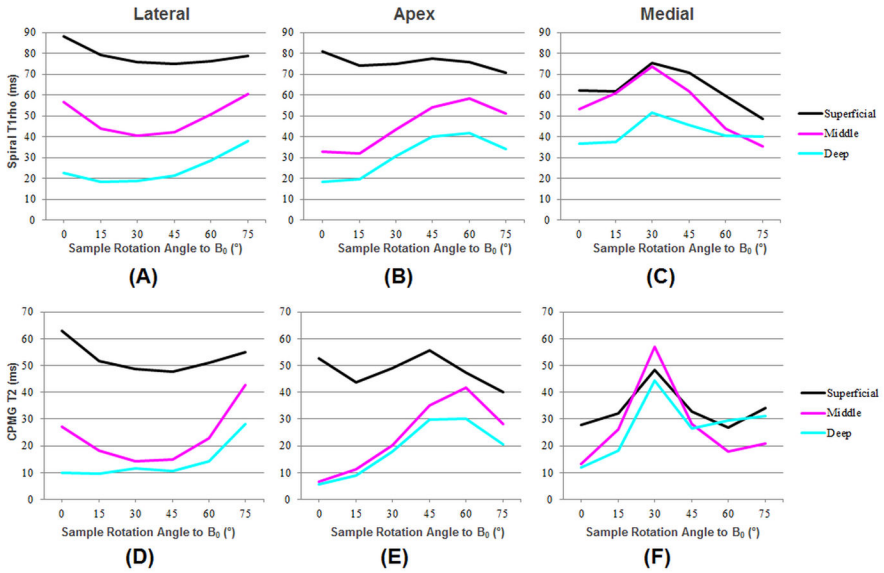


**Figure 3.**

Spiral T1rho profiles for the lateral (A), apex (B) and medial (C) regions including the superficial (black), middle (pink) and deep (blue) layers. CPMG T2 profiles for the lateral (D), apex (E) and medial (F) regions including the superficial (black), middle (pink) and deep (blue) layers. The angular dependence for both T1rho and T2 in patellar cartilage is apparent.

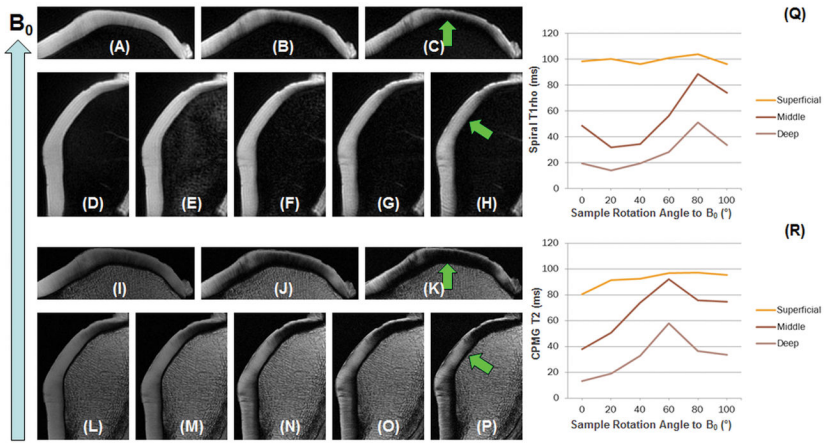


**Figure 4.**

Spiral T1rho imaging: apex parallel to $B_0$ with three TSLs of 0 (A), 20 (B) and 60 ms (C), and 60° relative to $B_0$ with five TSLs of 0 (D), 10 (E), 20 (F), 40 (G) and 80 ms (H). CPMG T2 imaging: apex parallel to $B_0$ with three TEs of 10 (I), 20 (J) and 60 ms (K), and 60° relative to $B_0$ with five TEs of 10 (L), 20 (M), 40 (N), 60 (O) and 80 ms (P). The regions indicated by the arrows show dramatic signal enhancement when the fibers are oriented at ~55° relative to $B_0$, consistent with strong magic angle effect for both T2 and T1rho relaxation. Superficial, middle and deep ROIs in the medial region (arrows) chosen for T1rho (Q) and T2 (R) analysis. Strong magic angle effects are seen in the middle and deep layers.

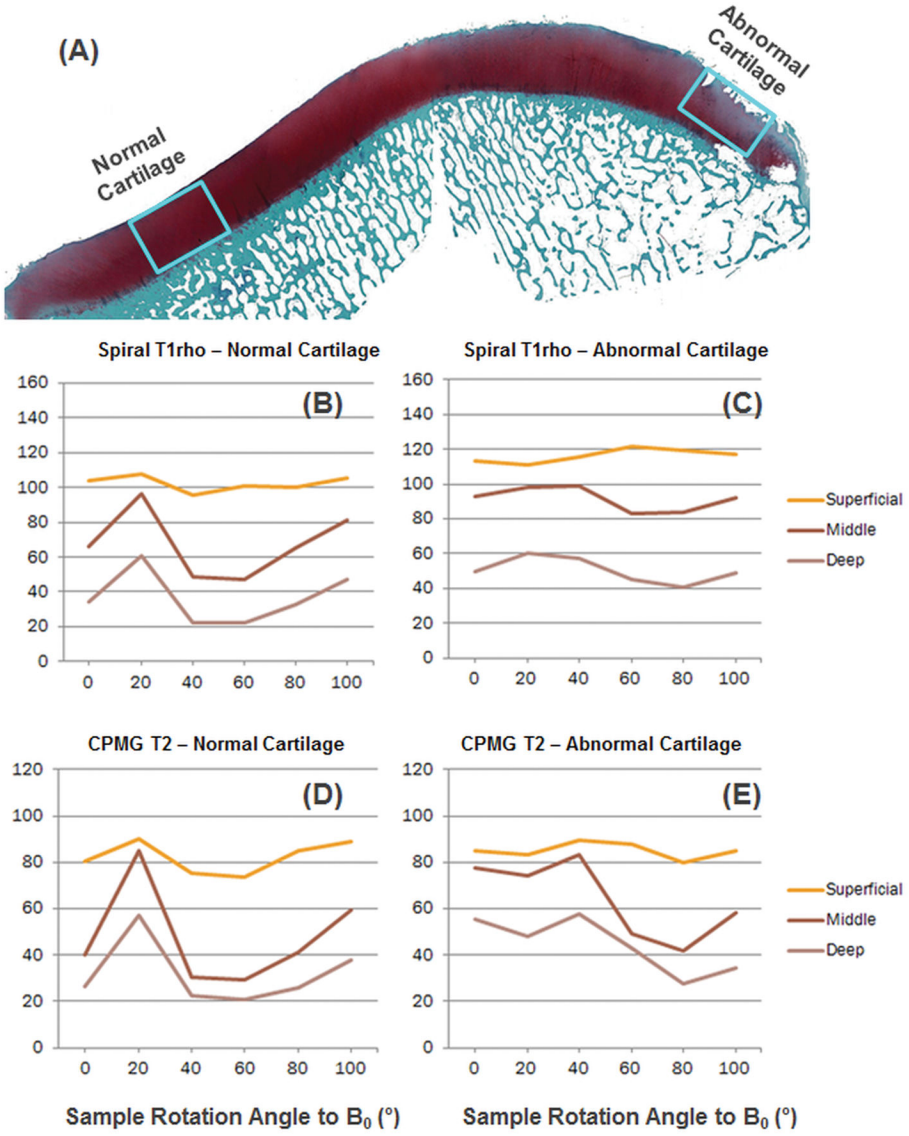


**Figure 5.**

Histology (A), spiral-T1rho and CPMG T2 for normal (H, J) and abnormal (I, K) cartilage indicate strong angular dependence.

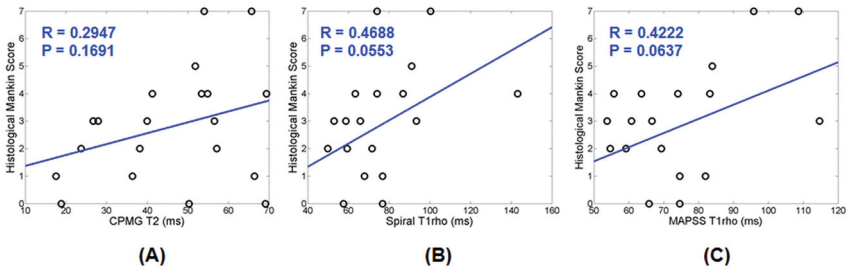


**Figure 6.**

Low to moderate correlation was seen between histopathologic grading (Mankin score) of patellar cartilage specimens and T2 (A), spiral T1rho (B), and MAPSS T1rho (C) values. A Mankin score of equal or less than 2 was considered normal, while a Mankin score of greater than 2 was considered abnormal.

**Table 1**

MR imaging protocol for articular cartilage from cadaveric human patellae.

| | FOV (cm) | TR (ms) | TE, T2 prep or TSL (ms) | Recon Matrix | Slice (mm) | BW (kHz) | Angular Orientations relative to B0 | Scan time (hours) |
|---|---|---|---|---|---|---|---|---|
| 2D Spiral T1ρ | 5 | 2000 | 0, 10, 20, 40, 80 | 256 × 256 | 2 | 125 | 0°, 20°, 40°, 60°, 80°, 100° | ~3 |
| 3D MAPSS T1ρ | 6 | 10 | 0, 10, 20, 40, 80 | 256 × 256 | 2 | 62.5 | 0°, 20°, 40°, 60°, 80°, 100° | ~3 |
| 2D CPMG T2 | 5 | 2000 | 10, 20, 30, 40, 50, 60, 70, 80 | 256 × 256 | 2 | 62.5 | 0°, 20°, 40°, 60°, 80°, 100° | ~3 |

**Table 2**

2D spiral T1rho, 3D MAPSS T1rho and CPMG T2 values and standard deviations in normal and abnormal patellar articular cartilage.

| | | Normal Cartilage | | | | Abnormal Cartilage | | | |
|---|---|---|---|---|---|---|---|---|---|
| | | **Superficial (10%)** | **Middle (60%)** | **Deep (30%)** | **Global ROI** | **Superficial (10%)** | **Middle (60%)** | **Deep (30%)** | **Global ROI** |
| 2D Spiral T1rho [ms] | Max | 105.7 ± 15.6 | 88.4 ± 11.8 | 59.2 ± 7.3 | 81.2 ± 12.4 | 109.7 ± 16.6 | 96.9 ± 12.1 | 66.4 ± 10.5 | 86.9 ± 14.0 |
| | Min | 86.6 ± 11.3 | 50.7 ± 9.4 | 23.5 ± 5.2 | 47.1 ± 10.1 | 88.7 ± 14.5 | 60.1 ± 7.3 | 24.8 ± 5.4 | 53.3 ± 12.8 |
| | Ratio | 123% | 174% | 252% | 172% | 124% | 161% | 268% | 163% |
| 3D MAPSS T1rho [ms] | Max | 114.9 ± 16.3 | 98.1 ± 13.6 | 65.1 ± 85.7 | 89.8 ± 11.7 | 134.0 ± 18.9 | 104.9 ± 13.5 | 69.3 ± 11.5 | 92.1 ± 13.7 |
| | Min | 94.1 ± 12.1 | 58.3 ± 10.9 | 27.4 ± 6.1 | 53.8 ± 10.6 | 105.2 ± 17.1 | 67.7 ± 12.8 | 28.8 ± 7.4 | 60.1 ± 11.6 |
| | Ratio | 122% | 168% | 238% | 167% | 127% | 155% | 241% | 153% |
| 2D CPMG T2 [ms] | Max | 85.3 ± 12.5 | 78.4 ± 13.0 | 55.1 ± 7.9 | 71.5 ± 10.3 | 93.7 ± 14.3 | 75.2 ± 12.6 | 53.4 ± 8.2 | 69.4 ± 11.4 |
| | Min | 66.6 ± 8.7 | 28.7 ± 8.7 | 21.4 ± 4.7 | 27.9 ± 6.6 | 66.2 ± 10.1 | 38.2 ± 9.4 | 17.6 ± 7.4 | 34.1 ± 8.8 |
| | Ratio | 128% | 273% | 258% | 256% | 142% | 197% | 303% | 204% |